Inorg. Chem. **2005**, *44*, 5286–5292

Solvation and Structure of $LiAlH_4$ in Ethereal Solvents

Damián E. Bikiel, Florencia Di Salvo, Mariano C. González Lebrero, Fabio Doctorovich,* and Darío A. Estrin*

Departamento de Química Inorgánica, Analítica y Química Física - INQUIMAE-CONICET, Facultad de Ciencias Exactas y Naturales, Universidad de Buenos Aires, Ciudad Universitaria, Pabellón 2, C1428EHA, Buenos Aires, Argentina

Received March 3, 2005

The nature of the solute species present in ethereal solutions of $LiAlH_4$ is of crucial importance for understanding the mechanisms for the reduction of ketones and other functional groups by $LiAlH_4$. We have employed a combination of theoretical and experimental techniques to investigate the structure of $LiAlH_4$ in ethereal solutions. Using complexation agents, we measured the IR spectra of $LiAlH_4$ and AlH_4^- in tetrahydrofuran (THF). Hybrid quantum-classical (QM-MM) simulations have also been carried out to compute the IR spectra of associated and dissociated $LiAlH_4$ species and the free-energy profile for the dissociation process in solution. Our experimental estimate of the dissociation constant in THF is 0.021 ± 0.002, while the predicted computational value corresponding to a model dimethyl ether solvent is 0.001. The free-energy profile shows only one minimum corresponding to a contact ion pair at a Li–Al separation distance of 3.0 Å. These results are consistent with the fact that $LiAlH_4$ is essentially associated in ethereal solutions forming contact ion pairs.

I. Introduction

The discovery of aluminum hydrides by Schlesinger and co-workers[1] in 1947 revolutionized organic synthesis by allowing the organic chemist to perform selective reductions that were not feasible previously. Since the early mechanistic proposals of Trevoy,[2] there have been several postulated reduction mechanisms involving different species. In some proposals, $LiAlH_4$ is supposed to remain associated, and in others, the reducing agent has been proposed to be a dimer.[3] Initially, it was suggested that the hydride was transferred from the free anion,[4] but later studies proposed that AlH_4^- is not the reducing agent.[5] In this sense, there have been several investigations that indicated that the cation played a significant role in the reaction. Several studies have been performed by sequestration of the cation; these studies were performed by adding various amounts of cations to the reaction mixture, changing the type of cation in the reaction mixture, or both.[5] It is still not clear if the reduction occurs prior to or in concert with the cation attack, but it is established that some sort of complexation of the carbonyl oxygen by lithium is necessary for the reaction to proceed.[6] The proposed mechanisms can be classified in two categories. In the first one (depicted in Scheme 1), the carbonyl oxygen is activated by the free-solvated cation, and then aluminum hydride (AlH_4^-) attacks the carbonyl carbon.[7]

Scheme 1. Dissociative Mechanistic Scheme

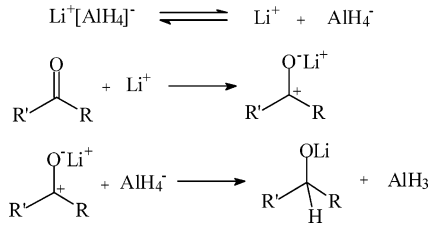

The second mechanism (depicted in Scheme 2) proposes a concerted attack of the whole $LiAlH_4$ molecule with no activation via dissociation of the cation.[8]

The relevance of both mechanisms is related to the dissociation equilibria between the associated ($LiAlH_4$) and

* To whom correspondence should be addressed. Phone: 54-11-4576-3378. Fax: 54-11-4576-3341. E-mail: dario@qi.fcen.uba.ar (D.A.E.); doctorovich@qi.fcen.uba.ar (F.D.).

(1) Finholt, A. E.; Bond, A. C.; Schlesinger, H. I. *J. Am. Chem. Soc.* **1947**, *69*, 1199.
(2) Trevoy, L. W.; Brown, W. G. *J. Am. Chem. Soc.* **1949**, *71*, 1675.
(3) Wiegers, K. E.; Smith, S. G. *J. Am. Chem. Soc.* **1977**, *99*, 1480.
(4) Brown, H. C.; McFarlin, R. F. *J. Am. Chem. Soc.* **1958**, *80*, 5372.
(5) Wiegers, K. E.; Smith, S. G. *J. Org. Chem.* **1978**, *43*, 1126.
(6) Ashby, E. C.; Boone, J. R.; Oliver, J. P. *J. Am. Chem. Soc.* **1973**, *95*, 5427.
(7) Ashby, E. C.; Boone, J. R. *J. Am. Chem. Soc.* **1976**, *98*, 5524.
(8) Luibrand, R. T.; Taigounov, I. R.; Taigounov, A. A. *J. Org. Chem.* **2001**, *66*, 7254.

10.1021/ic050330q CCC: $30.25
Published on Web 06/21/2005

Scheme 2. Concerted Mechanistic Scheme

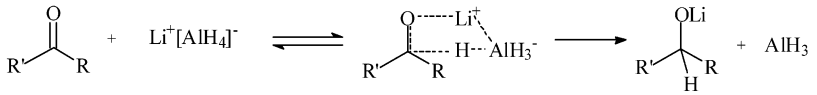

dissociated species ($Li^+ + AlH_4^-$). Precise information concerning the nature of the solute species arising from $LiAlH_4$ in ethereal solutions is necessary to rule out one of the mechanisms.

Although the crystal structure of $LiAlH_4$ was determined by X-ray studies and recently by neutron diffraction establishing the tetrahedral symmetry of AlH_4^-,[9] the nature of the species in solution has not been completely elucidated. Ashby et al. performed conductometric and ebulloscopic experiments in THF that were consistent with two concentration-dependent equilibria: an equilibrium between ion pairs and free ions at low concentrations (<0.1 *m*) and the formation of triple ions at higher concentrations (>0.4 *m*).[10] The reported value for the dissociation constant was 0.69×10^{-6} with an enthalpy of dissociation of -2.20 kcal/mol. A significantly larger value for the dissociation constant in THF of 0.11, obtained using calorimetric experiments, has been reported by Claudy et al.[11] The same authors reported an enthalpy of dissociation of 3.05 kcal/mol.

Structural information regarding the species in solution was obtained by employing spectroscopic techniques. Shriver et al. studied the IR and Raman spectra of $LiAlH_4$ with different solvents, temperatures, and concentrations.[12] They analyzed the observed spectra by assuming the existence of three distinct species in solution: ion pairs, tightly bound aggregates, and loosely bound aggregates.

$LiAlH_4$ has also been the subject of several theoretical investigations. The tetrahedral structure of the anion and the stability of the mono-, bi-, and tridentate coordinated conformations have been established by performing ab initio calculations in a vacuum.[13] The mechanism of reduction of formaldehyde and cyclohexanone has been investigated by performing DFT calculations in a vacuum.[8] The vibrational spectrum of AlH_4^- was also computed to assign an infrared matrix isolation spectrum.[14] Solvent and thermal effects on the structural properties were also explored.[15] Recently, ab initio studies on the crystal structure and phase diagram of $LiAlH_4$ have been reported because of the potential implication of this solid being used for hydrogen storage.[16]

The aim of this work is to shed light into the structural problem of the solvation of $LiAlH_4$ from a microscopic point of view. We focused on the relatively low concentration regime (<0.1 *m*), in which the fundamental reaction is the dissociation process. We performed a hybrid quantum-classical (QM-MM) simulation in which $LiAlH_4$ is treated quantum mechanically at the DFT level and a classical force field is used to model the ethereal solvent. We also predicted vibrational spectra and the free-energy profile for the dissociation process in ethereal solution. Computer simulation schemes have provided a valuable tool for the investigation of structural properties[17] and vibrational spectra in solution.[18] In addition, we also performed experiments by adding different amounts of 12-crown-6-ether to THF solutions of $LiAlH_4$ to obtain an estimate of the dissociation constant by complexing the Li cations and pushing the equilibrium toward dissociation.

II. Model and Simulation Methods

Our computational scheme was constructed by partitioning the system into quantum-mechanical (QM) and classical-mechanical (MM) subsystems. Considering a configuration of N_c atoms in the MM sub-system with coordinates and partial charges $\{R_l, q_l, l = 1, ..., N_c\}$ and N_q atoms in the QM sub-system with coordinates and nuclear charges $\{\tau_a, z_a, a = 1,..., N_q\}$, we propose the following expression for the ground-state Born−Oppenheimer potential energy surface that drives the dynamics of the nuclei:

$$E[\{R_i\}, \{\tau_\alpha\}] = E_{KS} + E_{QM-MM} + E_{MM} \quad (1)$$

where the first term is a purely QM piece given by the standard Kohn−Sham expression.[19] The second term in eq 1 accounts for the coupling of the QM and MM sub-systems and is given by

$$E_{QM-MM} = \sum_{l=1}^{N_c} q_l \int \frac{\rho(r)}{|r - R_l|} dr + \sum_{l=1}^{N_c} \sum_{\alpha=1}^{N_q} \left[v_{LJ}(|R_l - \tau_\alpha|) + \frac{q_l z_\alpha}{|R_l - \tau_\alpha|} \right] \quad (2)$$

where v_{LJ} is the Lennard-Jones potential between the classical and quantum part of the system and $\rho(r)$ is the electron density of the QM subsystem. The last term in eq 1 represents the potential energy contribution from the classical solvent potential treated with a single point charge potential.[20] For the QM region, computations were performed at the generalized gradient approximation (GGA) level using the BLYP combination of exchange and correlation functionals.[21−23] Gaussian basis sets of double-ζ plus polarization quality were employed for the expansion of the one-electron

(9) Hauback, B. C.; Brinks, H. W.; Fjellvåg, H. *J. Alloys Compd.* **2002**, *346*, 184.
(10) (a) Ashby, E. C.; Dobbs, F. R.; Hopkings, H. P., Jr. *J. Am. Chem. Soc.* **1973**, *95*, 2823. (b) Ashby, E. C.; Dobbs, F. R.; Hopkings, H. P., Jr. *J. Am. Chem. Soc.* **1975**, *97*, 3158.
(11) Claudy, P.; Bonnenot, B.; Mathurin, D.; Turck, G. *Thermochim. Acta* **1978**, *24*, 139.
(12) Shirk, A. E.; Shriver, D. F. *J. Am. Chem. Soc.* **1973**, *95*, 5904.
(13) Ramondo, F.; Bencivenni, L. *Chem. Phys.* **1991**, *158*, 1.
(14) Pullumbi, P.; Boutellier, Y.; Manceron, L. *J. Chem. Phys.* **1994**, *101*, 3610.
(15) Asciutto, E.; Crespo, A.; Estrin, D. A. *Chem. Phys. Lett.* **2002**, *353*, 178.
(16) (a) Vajeeston, P.; Ravindran, P.; Vidya, R.; Fjellvåg, H.; Kjekshus, A. *Phys. Rev. B* **2003**, *68*, 212101. (b) Løvvik, O. M.; Opalka, S. M. *Phys. Rev. B* **2004**, *69*, 134117.
(17) (a) Tuñon, I.; Rinaldi, D.; Ruiz-Lopez, M. F.; Rivail, J. L. *J. Phys. Chem.* **1995**, *99*, 3798. (b) Chalmet, S.; Harb, W.; Ruiz-Lopez, M. F. *J. Phys. Chem. A* **2001**, *105*, 11574. (c) Nagy, P. I. *J. Phys. Chem. A* **2002**, *106*, 2659. (d) Nemukhin, A. V.; Topol, I. A.; Grigorenko, B. L.; Burt, S. K. *J. Phys. Chem. B* **2002**, *106*, 1734.
(18) (a) Lynden-Bell, R. M.; Kosloff, R.; Ruhman, S.; Danovich, D.; Vala, J. *J. Chem. Phys.* **1998**, *109*, 9928. (b) Margulies, C. J.; Coker, D. F.; Lynden-Bell, R. M. *J. Chem. Phys.* **2001**, *114*, 367.
(19) Kohn, W.; Sham, L. J. *Phys. Rev. A.* **1965**, *140*, 1133.
(20) Jorgensen, W. L.; Chandrasekhar, J.; Madura, J. D.; Impey, R. W.; Klein, M. L. *J. Chem. Phys.* **1983**, *79*, 926.

orbitals.[24] The electronic density was also expanded in an auxiliary basis set;[24] the coefficients for the fit were computed by minimizing the error in the Coulomb repulsion energy. The use of this procedure results in an important speedup of the computations. To accurately describe the dissociation processes, we have incorporated a novel cutoff scheme in the QM-MM implementation of periodic boundary conditions, on the basis of the partitioning of the density, into our previously developed QM-MM code[25] (see Supporting Information for more details).

The classical potential used for the classical subsystem consisted of a three-point model used to describe alkyl ethers, specifically dimethyl ether (DME).[26] The DME model is similar electrostatically to other ether models, such as THF, but its implementation in the QM-MM code is computationally more efficient.

Molecular Dynamics Simulations. Initial configurations were generated from a preliminary 100 ps equilibration run, in which the quantum reactant was replaced by a classical rigid solute with partial charges obtained from a Mulliken population analysis. After the classical thermalization, the classical solute was replaced by a solute described at the QM level, according to the hybrid methodology described above. A second thermalization of 10 ps was performed for the hybrid system, and then the simulation was performed. The QM subsystems were solvated in a cubic box of size $a = 37.2$ Å using periodic boundary conditions[27] containing 497 DME molecules. We have performed constant temperature simulations,using the Berendsen thermostat, in which the average temperature of the sample is 300 K.[28] The equations of motion were integrated using the Verlet algorithm, with an integration step of 0.1 fs.[27] The SHAKE algorithm was implemented to handle intramolecular constraints in the solvent molecules.[29]

Free-Energy Profiles. The implementation of a simulation code to compute activation free-energy barriers that exceed the size of typical thermal fluctuations requires some kind of non-Boltzmann sampling procedure. In the present work, we resorted to a combination of molecular dynamics and umbrella sampling techniques.[30] We performed a series of simulation experiments over several, typically 10, adjacent windows, whose dynamics were governed by Hamiltonians that included, in addition to the QM-MM potential energy terms, an extra bias harmonic potential energy contribution of the form

$$V_i^{\text{bias}} = \frac{k_i}{2}(\xi - \xi_i)^2 \tag{3}$$

Eleven simulations were carried out along the reaction coordinate, which was chosen as the Li−Al distance. We used a box of 497 DME molecules with periodic boundary conditions. The system was thermalized to a temperature of 300 K using the Berendsen algorithm. To improve the simulation efficiency, we replaced the hydrogen atoms with deuterium atoms. This allowed us to employ a time step of 0.5 fs. We sampled the reaction coordinate from 2.0 to 6.0 Å and the harmonic constant ranged from 20 to 70 kcal/Å^2. Each simulation window was carried out for 30 ps. More technical details about the free-energy calculations are presented in the Supporting Information.

IR Spectra Simulation. The IR spectrum of a system can be predicted using different computational schemes. The usual method is to obtain the normal-mode frequencies and intensities from the diagonalization of the Hessian matrix. This method is useful for molecules in the gas phase. The inclusion of solvent effects can be achieved with continuum solvent models. However, this scheme may present flaws in cases in which there are strong specific solute−solvent interactions. The IR spectrum can also be computed directly from a molecular dynamics simulation using explicit solvent molecules. The infrared absorption $I(\omega)$ is related to the Fourier transform of the dipole autocorrelation function $C(t)$[31,32] by

$$I(\omega) = \frac{1}{2\pi}\int_{-\infty}^{+\infty} C(t)e^{-i\omega t}dt \tag{4}$$

The correlation function of a stationary property is independent of the time origin. This type of function depends on the interval between the correlated time values. In the discrete case, the dipole moment autocorrelation function $C(t)$ is then expressed by

$$C(\tau) = \frac{1}{T-\tau}\sum_{t_0=0}^{T-\tau-1} \mu(t_0)\mu(t_0+\tau) \tag{5}$$

where μ is the dipole moment at time t, T is the total number of time steps in the simulation, τ is the time interval, and t_0 is the time origin.

To obtain the spectrum of $LiAlH_4$ and AlH_4^- in DME, we simulated the systems (each quantum species in a box of 497 DME) using periodic boundary conditions and adjusting the density of the cage to the DME density. The simulation was carried out for 9 ps using a time step of 0.1 fs at a temperature of 300 K; a Berendsen algorithm was used for adjusting the temperature. The dipole moment was recorded for each step. The first derivative dipole moment autocorrelation function was obtained and Fourier transformed to obtain the vibrational frequencies and intensities of the system because it is more convenient to compute than the dipole moment autocorrelation function.

III. Experimental Methods

The motivation for the experiment was to obtain information about $LiAlH_4$ and AlH_4^-. We performed two types of experiments. In the first one, we changed the properties of the solution to force the association, while in the second one, we pushed the equilibrium toward dissociation.

All manipulations were performed under an argon or nitrogen atmosphere using standard Schlenk techniques or a drybox. Tetrahydrofuran (THF) and toluene (TOL) were distilled from Na/benzophenone under nitrogen just prior to use.

$LiAlH_4$, 12-crown-4 ether (CROWN), anhydrous 1,4-dioxane, and THF-d_8 were purchased from Sigma-Aldrich; THF was purchased from Merck, and TOL was purchased from Cicarelli. 12-Crown-4 ether was previously treated with 3 Å type-activated molecular sieves.

(21) Vosko, S. H.; Wilk, L.; Nusair, M. *Can. J. Phys.* **1980**, *58*, 1200.
(22) Lee, C.; Yang, W.; Parr, R. *Phys. Rev. B* **1988**, *37*, 785.
(23) Becke, A. D. *Phys. Rev. A* **1988**, *38*, 3098.
(24) Godbout, N.; Salahub, D. R.; Abdzelm, J.; Wimmer, E. *Can. J. Chem.* **1992**, *70*, 560.
(25) (a) González Lebrero, M. C.; Bikiel, D. E.; Elola, M. D.; Estrin, D. A.; Roitberg, A. E. *J. Chem. Phys.* **2002**, *117*, 2718. (b) Elola, M. D.; Laria, D.; Estrin, D. A. *J. Phys. Chem. A* **1999**, *103*, 5105. (c) Kohanoff, J.; Koval, S.; Estrin, D. A.; Laria, D.; Abashkin, Y. *J. Chem. Phys.* **2000**, *112*, 9498.
(26) (a) Jorgensen, W. L.; Ibrahim, M. *J. Am. Chem. Soc.* **1981**, *103*, 3976. (b) Chandrasekhar, J.; Jorgensen, W. L. *J. Chem. Phys.* **1982**, *77*, 5073.
(27) Allen, M. P.; Tildesley, D. J. *Computer Simulation of Liquids*; Clarendon Press: Oxford, U.K., 1987.
(28) Berendsen, H. J. C.; Postma, J. P. M.; van Gunsteren, W. F.; Di Nola, A.; Haak, J. R. *J. Chem. Phys.* **1984**, *81*, 3684−3690.
(29) Ryckaert, J. P.; Ciccotti, G.; Berendsen, H. J. C. *J. Comput. Phys.* **1977**, *23*, 327.
(30) Torrie, G.; Valleau, J. P. *J. Comput. Phys.* **1977**, *23*, 187.
(31) Noid, D. W.; Koszykowsi, M. L.; Marcus, R. A. *J. Chem. Phys.* **1977**, *67*, 404.
(32) Leach, A. R. *Molecular Modelling*, 2nd edition; Prentice Hall: New York, 2001.

Infrared spectra were recorded on a Nicolet Avatar 320 FTIR spectrometer with a Spectra Tech cell for liquids with CaF_2 windows. ^1H and ^7Li NMR spectra were obtained using a Bruker AM500 spectrometer equipped with a broadband probe, and the signals were referenced to TMS for ^1H NMR and to LiCl for ^7Li NMR. The lithium atomic absorption determination was made using SHIMADZU 6800 (Kyoto, Japan) spectrophotometer equipped with an ASC 6100 autosampler.

Li was measured by atomic absorptiometry in a solution obtained from 50 μL of $LiAlH_4$ saturated solution in THF diluted in water up to 25 mL to determine the concentration of the $LiAlH_4$ saturated solution in THF.

To perform the first type of experiment, we prepared solutions of $LiAlH_4$ in THF ($[LiAlH_4] = 0.5$ M as determined by ^1H NMR). After the mixture was centrifuged, the supernatant was divided into two equal parts. The first part was diluted with THF, and the second part was diluted with an equal volume of TOL (0.5 mL THF + 4 mL TOL). The aim of this experiment was to examine if a change in the shape of the spectra was detected by modifying the polarity of the solvent. By decreasing the solvent polarity, we tried to monitor spectral changes which may indicate a larger degree of association.

In the second type of experiment, we made mother solutions of $LiAlH_4$ in THF ($[LiAlH_4] = 0.3$ M as determined by Flame Spectroscopy) and used 12-crown-4 ether, a known Li^+ complexation agent, to push the equilibrium toward dissociation. We varied the $LiAlH_4$/CROWN ratio to measure the variation in the intensity of the bands that may indicate a larger degree of dissociation. The final $LiAlH_4$ concentration in the solutions was 0.1 M. This experiment allowed us to obtain the IR spectra of $LiAlH_4$ and AlH_4^-, the dissociation equilibrium constant (K_{dis}), and the complexation equilibrium constant of the CROWN with Li^+ in a THF solution (K_{comp})

$$K_{dis} = \frac{[AlH_4^-][Li^+]}{[LiAlH_4]} \quad (6)$$

$$K_{comp} = \frac{[Li^+CROWN]}{[Li^+][CROWN]} \quad (7)$$

IV. Results and Discussion

To study the association−dissociation equilibrium of $LiAlH_4$ in solution, we varied the polarity of the solvent by adding TOL to a THF solution. No significant differences between the spectra of the two solutions were observed, even up to a TOL/THF ratio of 8:1. This can be interpreted by assuming that the $LiAlH_4$ is already associated in the more polar solution, the change in the polarity is too small to induce any change in the dissociation equilibrium, or both.

On the other hand, the addition of CROWN to a THF solution of $LiAlH_4$ modified the position and shape of the band at 1693 cm^{-1} in the $LiAlH_4$/THF spectrum to a unique band at 1650 cm^{-1} in $LiAlH_4$/THF/CROWN spectrum. This result can be explained by assuming a complete displacement of the dissociation equilibrium to the dissociated species in the presence of an excess of CROWN because it coordinates to lithium with a high equilibrium constant. By adding of different amounts of CROWN, we forced the equilibrium position, allowing the observation of different species ratios. The experimentally obtained spectra are shown in Figure 1.

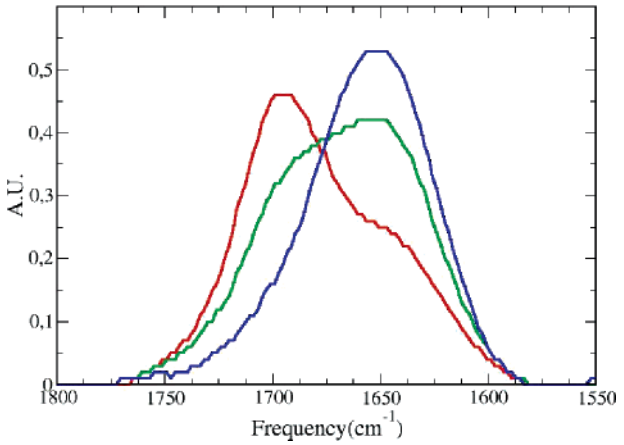

Figure 1. Experimental IR spectra in THF. Each spectrum corresponds to a different $LiAlH_4$/CROWN ratio. The spectra are 0.1 M $LiAlH_4$ (red line), 0.1 M $LiAlH_4$ + 0.06 M CROWN (green line), and 0.1 M $LiAlH_4$ + 0.16 M CROWN (blue line).

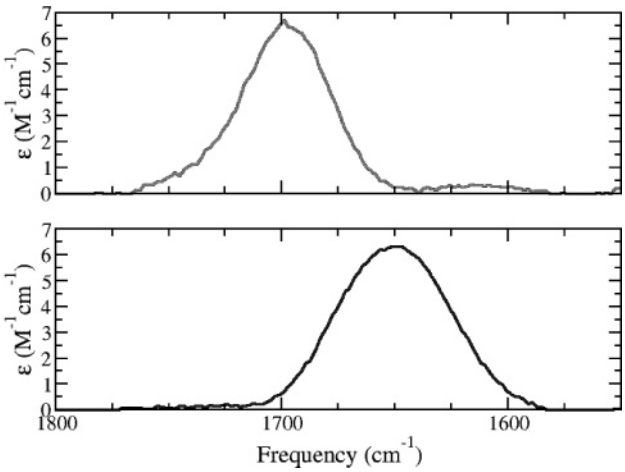

Figure 2. Experimental spectra for AlH_4^- (bottom panel) and $LiAlH_4$ (upper panel).

Using the data obtained from these experiments, we analyzed the relative concentrations of the different species in each experiment to obtain an estimate of the dissociation constant. We used an iterative procedure based on minimizing the square differences between different experimental and calculated values (see Supporting Information for details). The results of this procedure were the absorption spectra for pure $LiAlH_4$ and AlH_4^- and the values of the two constants. The decomposition of the experimental spectra in the absorption spectra of the $LiAlH_4$ and AlH_4^- after the minimization procedure are shown in Figure 2.

Because the complexation constant for CROWN and Li^+ in THF (K_{comp}) has not been determined, we used as a first guess a value obtained for other solvents[33,34] by extrapolating $\log(K_{comp})$ according to the polarity. We could estimate a value for $\log(K_{comp})$ of ~2 for THF that corresponds to a value for the complexation constant of 232 ± 28. For the dissociation constant, we found a value of 0.021 ± 0.002 that corresponds to a $\Delta G°$ of 2.31 ± 0.06 kcal/mol. The observation of an isosbestic point in Figure 1 is indicative

(33) Poonia, N. S.; Bajaj, A. V. *Chem. Rev.* **1979**, *79*, 389.
(34) Izatt, R. M.; Bradshaw, J. S.; Nielsen, S. A.; Lamb, J. D.; Christensen, J. S. *Chem. Rev.* **1985**, *85*, 271.

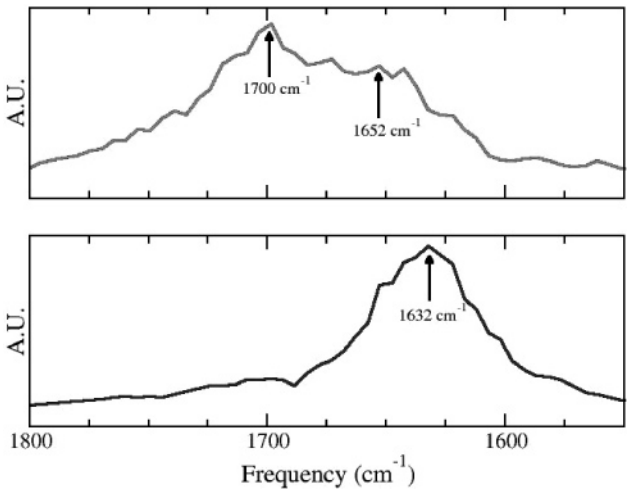

Figure 3. Computed IR spectra for AlH_4^- (bottom panel) and $LiAlH_4$ (upper panel).

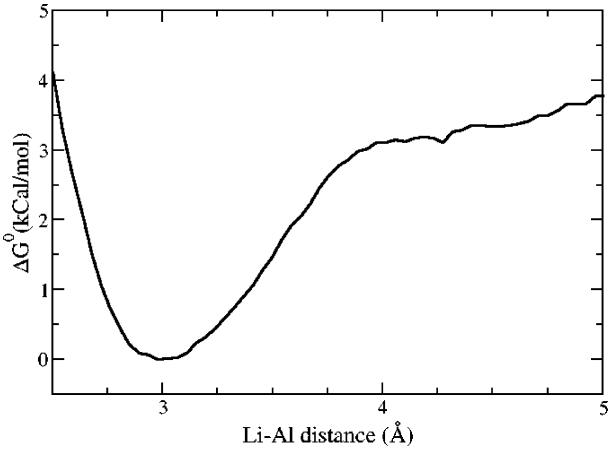

Figure 4. Computed free-energy profile for the dissociation process.

of an equilibrium between two species. Using this indication and the fact that the concentration is 0.1 M, we assume that there is not appreciable formation of triple ions in our experiments and that only the dissociation process is operative in this range of concentrations.

The spectra obtained from the fitting procedure indicates that, in the first place, the AlH_4^- spectrum shows only one band at 1650 cm^{-1}. This fact is consistent with the tetrahedral geometry of AlH_4^- and the observation that the addition of CROWN moves the shoulder-type spectrum to an unique band because of dissociation. In the second place, the spectrum of $LiAlH_4$ shows two definite bands. The first is located at 1693 cm^{-1}, while the second, less intense than the first, is located at 1613 cm^{-1}. These results allowed us to understand the spectral features of $LiAlH_4$ in a THF solution. The shoulder in the experimental spectrum of $LiAlH_4$ in THF is probably caused by both species, $LiAlH_4$ and AlH_4^-. The sum of the three bands would produce a shoulder at 1650 cm^{-1} and a band at 1693 cm^{-1}. The computed spectra (Figure 3) are in reasonable agreement with the experimental spectra.

The computed spectrum for $LiAlH_4$ shows two bands at about 1700 and 1652 cm^{-1}. The band at 1700 cm^{-1} is in agreement with the experimental value, but the second band is displaced almost 40 cm^{-1} to higher frequencies. In the experimental spectrum, the intensity ratio of the 1700 cm^{-1}/1652 cm^{-1} bands is close to 16, and in the simulated spectrum, the intensity ratio is only approximately 2. This is probably a result of the fact that the computed spectrum corresponding to $LiAlH_4$ corresponds to a variety of solvation situations not completely representative of the experimental situation because of the short simulation times and the fact that the time scale for the solvation−desolvation phenomena is in the order of the simulation time. It is important to notice that, in our simulation, we did not observe any dissociation event. The structural details in the solvent model may also partially account for the observed differences. This also points to the existence of subtle solvation effects, which may be responsible for the variations observed in the spectral features of $LiAlH_4$ in similar solvents found by Shriver et al.[12] The AlH_4^- calculated spectrum is in good agreement with the experimental spectrum. Only one band at 1632 cm^{-1} is observed, compared to the band at 1650 cm^{-1} that is observed in the experimental.

It is important to note that the real spectrum of $LiAlH_4$ in solution would be a superposition of the two fitted spectra. Because the simulation of $LiAlH_4$ was short, the entire configuration space was not completely explored. With a sufficiently large simulation, some dissociation events must have been observed, and these events must contribute to the final spectrum of $LiAlH_4$. The two spectra correspond to an extreme situation of the solvation structure of $LiAlH_4$.

The simulations show that the spectrum of $LiAlH_4$ in solution is compatible with an equilibrium displaced to the associated species. The computed free-energy profile for the dissociation process is shown in Figure 4. We have only observed one minimum, corresponding to a contact ion pair. The coordination number for lithium in the contact ion pair is 3. More solvent molecules are able to become closer to lithium upon dissociation, and indeed, a coordination number of 4 is observed for Li−Al separations larger than 3.5 Å. Snapshots showing the first coordination shell of $LiAlH_4$ at different Li−Al separations are depicted in Figure 5. As can be seen from the computed profile, solvent-shared ion pairs, in which the ionic constituents of the pair are separated by only a single solvent molecule, are not stable local minima, as has been observed, for example, from the dissociation of NaCl in an aqueous solution.[33] However, a full range of Li−Al separations are accessible thermally because of the small free-energy difference between the contact and the solvent-separated ion pairs.

Our calculations for isolated $LiAlH_4$ show a Mulliken charge on the Li atom of 0.29 *e* and a Li−Al distance of 2.50 Å. On the other hand, the minimum in the free-energy profile corresponds to a Li−Al distance of 3.0 Å, significantly larger than the optimized value in a vacuum. The mean value of the Mulliken charge on Li corresponding to the minimum free energy is 0.70 ± 0.04 *e*. These differences are indicative that there is a much larger degree of ionic character in solvated $LiAlH_4$, which may be considered a contact ion-pair, compared to that of the essentially covalent isolated species.

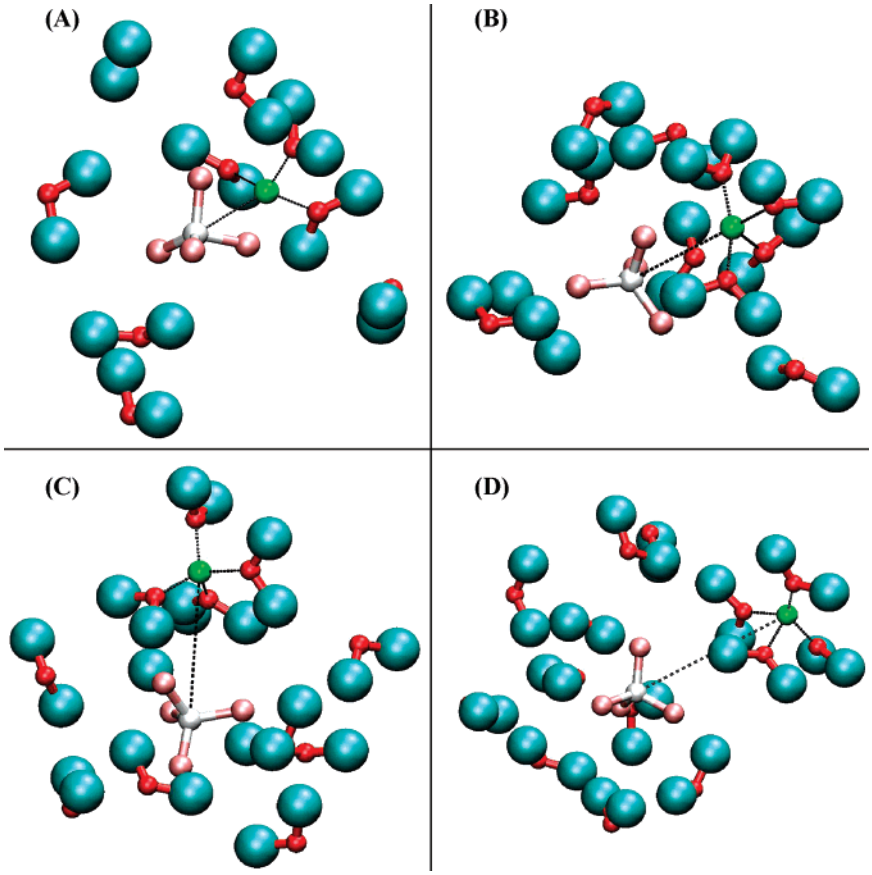

Figure 5. Snapshots of configurations of solvated $LiAlH_4$ showing only solvent molecules in the first solvation shell corresponding to different windows of the umbrella sampling simulation. Snapshots corresponding to the Li−Al distances of 3.0, 4.0, 5.5, and 6.0 Å are depicted in panels A, B, C, and D, respectively.

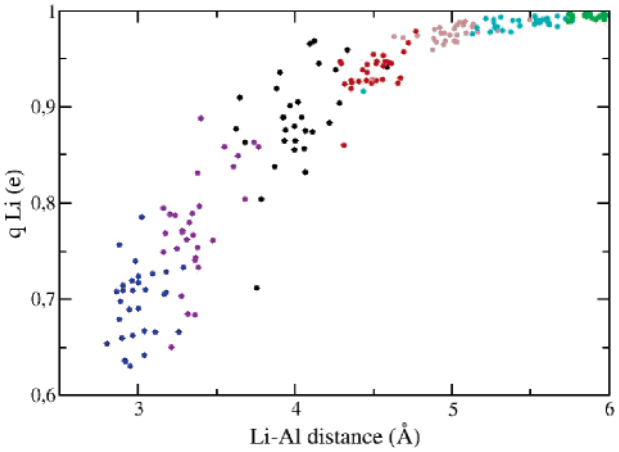

Figure 6. Mulliken Li charges versus Li−Al distance obtained from the umbrella sampling simulation.

In Figure 6, we represent the Li Mulliken population as a function of the Li−Al distance obtained from plotting the charges of selected snapshots in the umbrella sampling simulations. At the Li−Al = 3.0 Å window (Figure 5A), the Li atom is solvated most of the time by three solvent molecules. At the Li−Al distance of 4.0 Å, the snapshot is still corresponding to a contact ion pair (Figure 5B), but because of the larger Li−Al separation, Li is able to accommodate 4 solvent molecules in its coordination shell. This is consistent with the fact that the Li Mulliken charge is significantly larger. There were no events in which the so-called solvent-shared ion pair (in which one solvent molecule is coordinating both the anion and the cation) is formed in this range of distances. In the snapshot corresponding to the Li−Al distance of 5.5 Å (Figure 5C), some solvent molecules are found to solvate both Li and AlH_4^- forming a solvent-shared ion pair. The positive methyl groups are oriented toward the negative hydrogen atoms of AlH_4^-, while the oxygen is directed toward the Li cation. However, because the charge on the anion is delocalized, solvation is not directional and its coordination structure is very loose. The snapshot of the Li−Al distance of 6.0 Å (Figure 5D) corresponds to the onset of the formation of a solvent-separated ion pair.

It is interesting to note that, unlike what happens, for example, with the aqueous solvation of NaCl for which the solvent-shared ion pair corresponds to a secondary minimum in the free-energy profile,[35] we did not find that solvent-shared ion pairs correspond to a minimum in the free-energy profile, probably because of the charge delocalization of AlH_4^- and the less polar nature of ethereal solvents. In fact, the only minimum corresponds to the associated species (contact ion pair), with a $\Delta G°$ for dissociation of about 4 kcal/mol, in reasonable agreement with the experimental value. This difference in free energy corresponds to an equilibrium constant of about 0.001, a result consistent with the experimental estimation.

(35) Smith, D. E.; Dang, L. X. *J. Chem. Phys.* **1993**, *100*, 3757.

V. Conclusions

In this work, we explored the structure of $LiAlH_4$ in ethereal solutions. Computer simulations and experimental results are consistent with a dissociation equilibrium displaced to the associated species. However, a significant amount of the dissociated species is also expected to exist. The simulated spectra were consistent with the experimental ones. From the simulations, we can conclude that the free-energy difference in a dimethyl ether model solvent between associated and dissociated species is about 4 kcal/mol. This value is consistent with the experimental estimate in THF of 2.31 ± 0.06 kcal/mol, corresponding to the computationally and experimentally estimated equilibrium constants for the dissociation of approximately 0.001 and 0.021 ± 0.002, respectively. Our results are consistent with previous thermochemical investigations, which predicted a dissociation constant of 0.11 in THF.[11] The most important feature in the free-energy profile of the dissociation process of $LiAlH_4$ is the fact that only one minimum is observed. This minimum corresponds to the contact ion pair. The values of the charges of this contact ion pair are larger than those calculated in a vacuum, showing that a significant polarization is achieved in solution. Partially dissociated, completely dissociated, or both configurations may also be populated at room temperature because of the small free-energy difference between the associated and dissociated species. Our results indicate that the predominant species at room temperature is the contact ion pair. However, this does not necessarily imply that the reduction mechanism depicted in Scheme 2, in which the reducing agent is the associated species, will be the operative one. Further investigations of the reaction profiles for both schemes are required to settle this issue.

Acknowledgment. This work was partially supported by the University of Buenos Aires, ANPCyT (Project PICT 06-08447), CONICET (PIP 02508), and Fundación Antorchas.

Supporting Information Available: Details of the QM-MM implementation, validation of the DFT scheme, and experimental spectra fitting procedure. This material is available free of charge via the Internet at http://pubs.acs.org.

IC050330Q